SYNAPSE 28:271–279 (1998)

Synapse-Specific Accumulation of Lithium in Intracellular Microdomains: A Model for Uncoupling Coincidence Detection in the Brain

ANATOLII Y. KABAKOV,[1,4] NIKOLAS B. KARKANIAS,[3,4] ROBERT H. LENOX,[1,2,3] AND ROGER L. PAPKE[1,3]
[1]*Department of Pharmacology and Therapeutics, University of Florida Medical College, J.H. Miller Health Center, Gainesville, Florida*
[2]*Department of Psychiatry, University of Florida Medical College, J.H. Miller Health Center, Gainesville, Florida*
[3]*Department of Neuroscience, University of Florida Medical College, J.H. Miller Health Center, Gainesville, Florida*
[4]*The first and second authors contributed equally to this work.*

KEY WORDS bipolar disorder; glutamate receptor; dendritic spine; ion diffusion

ABSTRACT Lithium's therapeutic specificity for the treatment of bipolar disorder may be attributable in part to an ability to target sites where there are high levels of synaptic activity. We show that glutamate receptors expressed in oocytes are highly permeable to lithium. Mathematical simulations of Li^+ diffusion in mature dendritic spines suggest that in the presence of 1 mM extracellular lithium one synaptic current can increase Li^+ concentration in the spine head by 4 mM with a decay time constant of about 15–20 ms. Two or more current spikes will produce oscillations between 6 and 8 mM or potentially higher. These results predict that the local intracellular lithium in dendritic spines can rise to high enough levels to uncouple second messenger mechanisms of coincidence detection. **Synapse 28:271–279, 1998.**

INTRODUCTION

Bipolar disorder, formerly known as manic-depression, affects approximately 1% of the US population and represents a serious public health problem (Keller and Baker, 1991). Treatment with lithium salts has proven the most effective therapy for bipolar disorder (Lenox and Manji, 1995; Lenox et al., 1997). Lithium has many effects within the cell, and while the precise mechanisms that underlie the therapeutic actions of lithium are still unclear, lithium is known to affect several G-protein-coupled signal transduction systems (Lenox and Manji, 1995; Manji et al., 1995), such as the second messengers derived from phosphoinositide (PI) signaling, specifically IP_3 and DAG, which are generated from the hydrolysis of membrane-bound phosphatidylinositol 4,5, bisphosphate (PIP_2). At submillimolar concentrations, lithium (but not other monovalent cations) is known to uncompetitively inhibit myo-inositol-1-phosphatase (EC_{50} = 0.8 mM) (Hallcher and Sherman, 1980), a key enzyme involved in recycling inositol into the membrane for the regeneration of PIP_2. Higher concentrations of lithium (approx. 5 mM) will also inhibit receptor mediated signaling within the adenylate and guanylate cyclase systems and subsequent generation of cyclic AMP and cyclic GMP (Kanba et al., 1991; Ebstein et al., 1980).

The homeostatic regulation of intracellular lithium concentration is a balance of active and passive processes which parallel and interact with the systems that regulate other intracellular ions such as sodium, potassium, calcium, and bicarbonate. The extracellular (i.e., serum) concentration of lithium attained during the therapeutic use of lithium salts can be easily measured, and is in the range of 1 mM (Lenox and Manji, 1995; Lam and Christensen, 1992; Gani et al., 1993). However, intracellular concentrations of lithium are crucial for predicting physiological effects. Intracellular concentrations in the brain are relatively difficult to evaluate, but averaged over large samples of tissue have been estimated to also be in the range of 0.5–1.0 mM (Lam and Christensen, 1992; Gani et al., 1993). The passive electrochemical handling of lithium disposition across the membrane would predict tenfold higher intracellular concentrations due to the cell's resting negativity. Therefore, it is clear that lithium concentrations in the brain are not at equilibrium.

There are several paths by which lithium may enter a cell, including through ligand-gated ion channels, which would provide routes for Li^+influx in a brain region-specific manner, based on the selective expression of neurotransmitter receptor subtypes. Influx through these pathways would not only be rapid, but synchro-

*Correspondence to: Roger L. Papke, Ph.D., Department of Pharmacology & Therapeutics, P.O. Box 100267, University of Florida, Gainesville, FL 32610.

Received 30 January 1997; accepted 31 July 1997.

nized both temporally and spatially to synaptic activity. Such activity-dependent local heterogeneity of lithium concentrations is difficult to measure directly, but we can calculate the lithium diffusion from the synapse area to the dendrite body by using experimentally determined values for lithium permeability through glutamate receptor subtypes and applying those data to a simulation of diffusion within a synaptic spine. The concentration of lithium averaged over the entire neuron might be modest, while local concentrations in the dendritic spines become significantly elevated and thereby alter the relative balance of second messenger systems that are critical to triggering long-term events associated with neuronal plasticity.

In this study, we estimated the lithium component of glutamate-activated current through ionotropic glutamate receptors using heterologous expression and two electrode voltage clamp techniques in Xenopus oocytes. Then we applied these data to a mathematical simulation of lithium diffusion in the dendritic spine by using published parameters of spine geometry (Barbour et al., 1994; Spacek and Harris, 1997) and synaptic current (Vyklicky et al., 1991). Our results confirm that 1 mM extracellular Li^+ can lead to intracellular levels sufficient to profoundly alter the second messenger-mediated coincidence detection in dendritic spines associated with the activation of glutamate receptors under physiological conditions. Preliminary results have been published in abstract form (Karkanias et al., 1995; Kabakov et al., 1997).

RESULTS

Electrophysiology

We obtained data on all three classes of glutamate receptors, AMPA-selective, kainate-selective, and NMDA-selective. In all cases, lithium appears to be approximately equally permeable as sodium; however, the macroscopic conduction differs among the subtypes.

AMPA-selective receptors: GluR1, GluR1 +GluR2, and GluR3

The permeability and conductance of lithium through various AMPA receptor subtypes were examined by applying voltage ramps during the plateau phase of an agonist response. Current–voltage relationships (Fig. 1) were obtained in both control Ringer (115 mM sodium) and lithium-Ringer (115 mM lithium substituted for sodium).

From these results we see that subunit composition plays a key role in determining lithium conduction, though not its relative permeability. The I–V relationship for the GluR1 (Fig. 1A) and GluR1 + R2 (Fig. 1C) receptors displayed no shift in reversal potential, indicating that (compared to potassium) the relative permeability of lithium is equal to sodium for these receptor types. In these experiments, equilibration times with the extracellular lithium-Ringer were relatively short (2 min), so that little lithium uptake by the oocyte should occur and the equilibrium potential for lithium remained high, comparable to that for sodium.

While both GluR1 and GluR1 + R2 receptor subtypes show equal permeability for lithium (compared to sodium), they show striking differences in the conductance or slope of the I–V relations. Specifically, while for GluR1 sodium and lithium appear to have both similar permeability and conductance, conductance increases in lithium when the GluR2 subunit is present. This result suggests that the expression of GluR2 results in receptors that may effectively target a synapse for local increases in lithium, which is likely to be important for the synaptic receptors of specific neuronal subpopulations in the hippocampus.

The GluR3 channel resembles GluR1 in calcium permeability and inward rectification. However, the macroscopic conductance of GluR3 homomeric receptors in the presence of lithium was greatly increased compared to conduction in sodium. The currents for GluR3 were approximately 2.8 times larger in the presence of high lithium (Fig. 1B).

Kainate-selective receptors: GluR6(R) and GluR6(Q)

The permeability and conductance of lithium through concanavilin A treated GluR6(Q) and GluR6(R) receptors were also evaluated and showed somewhat smaller macroscopic conductance in lithium compared to sodium (see Fig. 1D for representative GluR6(Q) trace). Although macroscopic conductance was reduced in high extracellular lithium, these receptors were equally permeant to lithium (compared to sodium), as indicated by the lack of a reversal potential shift when the primary extracellular ion was exchanged (Fig. 1D).

NMDA-selective receptors: NMDAR1 + NMDAR2a and NMDAR1 + NMDAR2b

The NMDAR1 + NMDAR2a and NMDAR1 + NMDAR2b subunit combinations were evaluated for their relative permeability and macroscopic lithium conduction. While for both receptor subtypes lithium permeability was comparable to that of sodium, the macroscopic conduction was less for both. A representative current–voltage relationship for NMDAR1 + NMDAR2a is shown in Figure 1E.

Macroscopic conduction and permeability

These experiments measure macroscopic conduction (g), where $g = NP_{open}\gamma$ (N = total number of channels, P_{open} = proportion of channels open, and γ = conductance of a single channel). For any given cell over the duration of the experiment, N may be considered a constant, and so a change in conductance must represent either a change in P_{open} or in γ. Note that for the

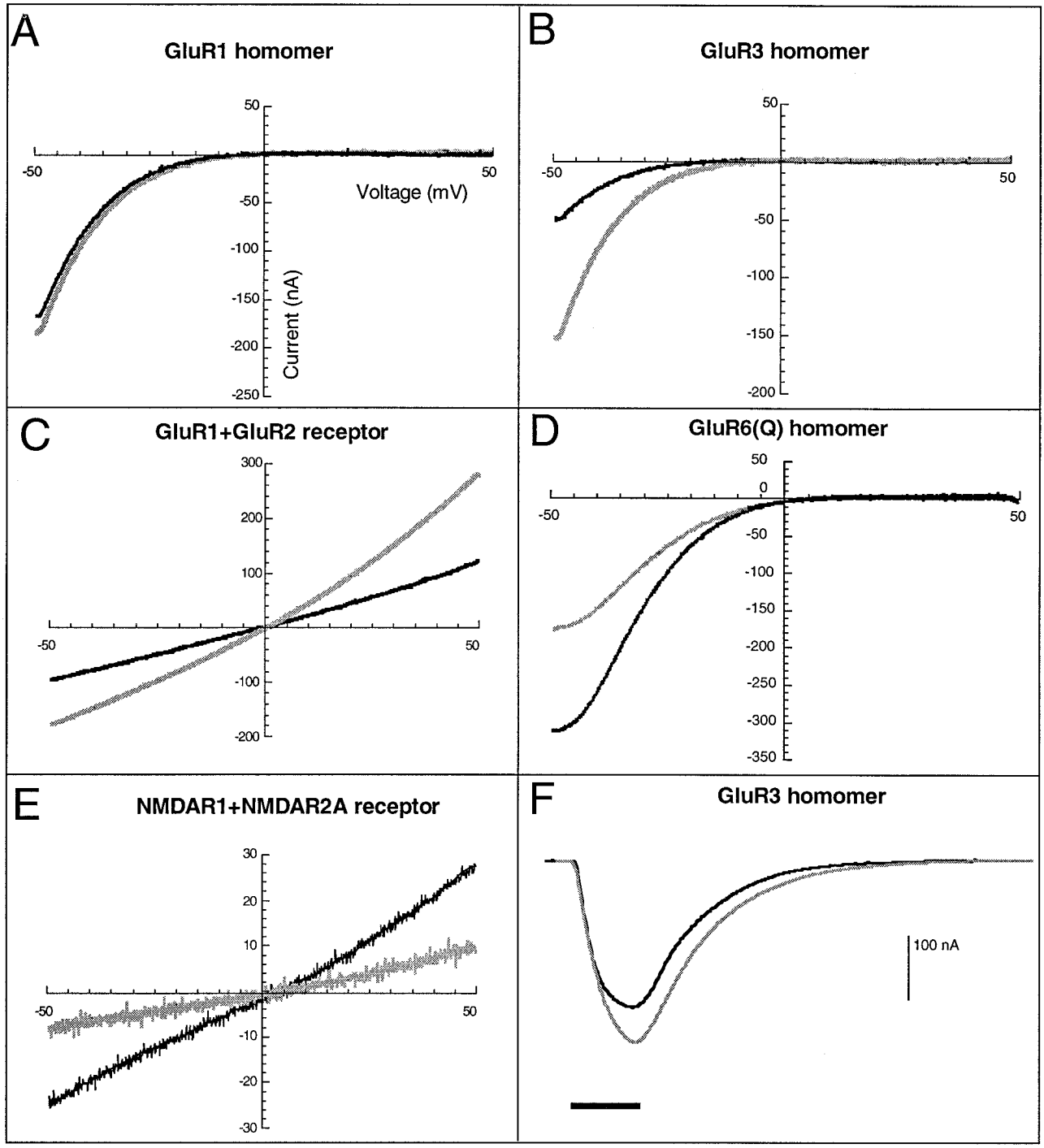

Fig. 1. Glutamate receptor current–voltage relationships in sodium and lithium. Shown are the current–voltage relationships for five different glutamate receptor subtypes generated from voltage ramps applied during periods of sustained agonist application. To calculate the receptor-specific current–voltage relationships, we subtracted out passive membrane responses to the same voltage ramps applied in the absence of agonist. The current–voltage relationships obtained in normal (sodium) Ringer are plotted as black lines, and those obtained in lithium-Ringer are plotted as gray lines. In panel **F** the data plotted by the gray line represents a whole oocyte response obtained in 5 mM lithium-Ringer. (A) The I–V relationship of GluR1 homomeric receptors. (B) The I–V relationship of GluR3 homomeric receptors. (C) The I–V relationship of GluR1 + GluR2 heteromeric receptors. (D) The I–V relationship of GluR6(Q) homomeric receptors. (E) The I–V relationship of NMDAR1+ NMDAR2a heteromeric receptors. (F) Representative traces illustrating the effect of 5 mM lithium on the macroscopic response of GluR3 expressing oocytes to 100 μM kainate. Control responses (black line) were obtained in normal (115 mM Na^+) Ringer, and then the extracellular solution was exchanged for Ringer containing 5 mM Li^+ (plus 110 mM Na^+, gray line). The scale bar is 100 nA and the duration of each trace is 2 min. The period of agonist application is indicated by the bar below the traces.

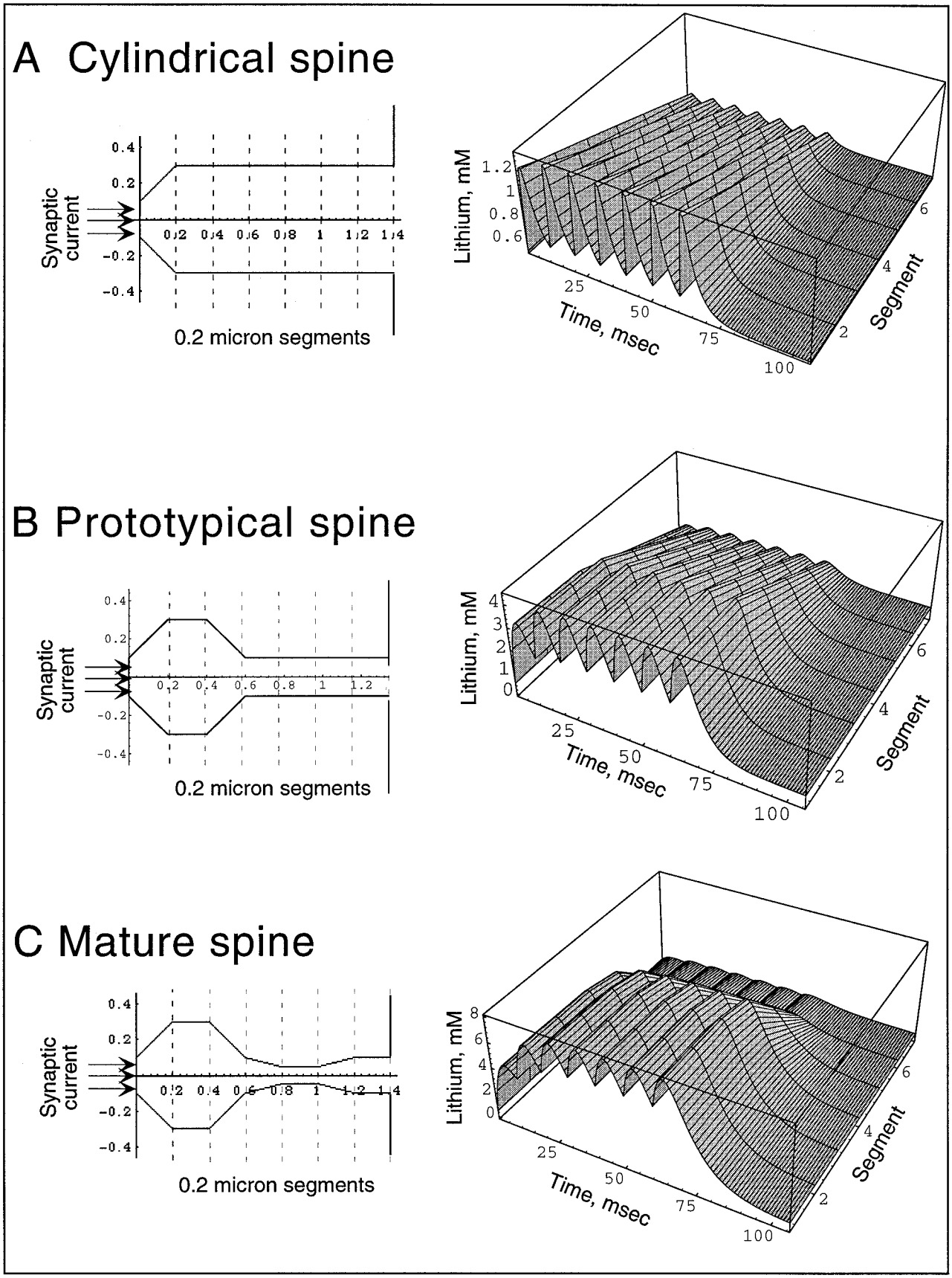
A Cylindrical spine
Synaptic current
0.4
0.2
-0.2
-0.4
0.2 0.4 0.6 0.8 1 1.2 1.4
0.2 micron segments
Lithium, mM
1.2
1
0.8
0.6
25
50
75
100
Time, msec
2
4
6
Segment
B Prototypical spine
Synaptic current
0.4
0.2
-0.2
-0.4
0.2 0.4 0.6 0.8 1 1.2
0.2 micron segments
Lithium, mM
4
3
2
1
0
25
50
75
100
Time, msec
2
4
6
Segment
C Mature spine
Synaptic current
0.4
0.2
-0.2
-0.4
0.2 0.4 0.6 0.8 1 1.2 1.4
0.2 micron segments
Lithium, mM
8
6
4
2
0
25
50
75
100
Time, msec
2
4
6
Segment

Fig. 2

GluR1 + GluR2 subunit combination, the I–V relationship has an increased slope in the presence of lithium for both the inward and the outward arms of the relationship. However, under these experimental conditions outward currents should be carried by potassium (as in the control condition), not lithium, so the single channel conductance should not differ in this voltage range. This suggests that the increase in macroscopic current may then be due to a change in channel activation probability rather than single channel conductance. While it will be of interest to study the effects of low lithium concentrations on channel activation in detail (Karkanias and Papke, in preparation), of most relevance to the present analysis is the observation that lithium will permeate the glutamate receptors equally well as sodium.

Extrapolations between conditions of high and low extracellular lithium

Although complete substitution of lithium for sodium represents a strictly experimental condition, this method provides the most sensitive assessment of the essential biophysical properties of the channel, and this assessment is applicable for channel function in vivo under physiological conditions. Our preliminary studies with low extracellular lithium (Karkanias and Papke, in preparation) suggest that lithium components of synaptic currents should roughly scale as the mole fraction of lithium in the extracellular solution. Specifically, glutamate receptors that have reduced macroscopic conduction in high extracellular lithium (e.g., GlurR6 and NMDAR1) showed no anomalous reductions in current when extracellular lithium was reduced to the range of 1–5 mM. However, interestingly, a significant ($P < 0.05$) potentiation of GluR3 responses remained when the extracellular lithium was reduced to 5 mM (Fig. 1F). After 5 min in the presence of 5 mM Li^+ and 110 mM Na^+, responses to 100 μM Kainic acid were 25 ± 5% larger than those of cells retained in 115 mM Na^+ (n = 10 in each group).

Computer simulations of local lithium concentration domains

Alterations of lithium concentration in a dendritic spine head is a result of lithium currents through the post-synaptic membrane and lithium diffusion in intracellular space. The most significant factors for our model are the lithium component of the synaptic current and lithium diffusion from the spine to the dendrite body. Note that in our simulations we assumed that the local lithium concentration domains are small and the temporal windows relatively brief. These assumptions permitted us to ignore the extrusion rates of lithium.

Estimation of the lithium component of synaptic current

We may make a first approximation of the contribution of any particular extracellular cation in the synaptic inward current as being proportional to its extracellular mole fraction, the electrochemical driving force, and the conductivity and P_{open} of activated channels for this cation. In our case, the synaptic current is carried mostly by the main extracellular cation, sodium, the concentration of which is ≈144 mM. The therapeutic concentration of extracellular lithium as reflected in plasma of bipolar patients is in the range of 0.8–1.2mM (Gelenberg et al., 1989). Our experimental data indicate that the relative conductivity of glutamate receptors for lithium may differ from that for sodium, ranging from 0.5 for NMDA receptors to 2.8 for GluR3 receptors (Fig. 1). However, in all cases the relative permeability for lithium was the same as for sodium. We take the equivalence in permeability to be a more significant factor under the physiological conditions of relatively low extracellular lithium than the apparent effects on whole cell conduction. Based on molar fraction, this would suggest a 0.7% lithium component to the synaptic current. Yet the nature of lithium's effect on macroscopic conduction should not be ignored, since it appeared that for the predominant non-NMDA receptors there may be a general increase in P_{open}, suggesting that the total synaptic currents would be larger. Preliminary data indicate that this effect may also occur at low lithium concentrations for specific receptor subtypes (Karkanias and Papke, in preparation), which would have the effect of increasing both sodium and lithium influx. Therefore, to estimate the lithium component (0.7%) of potentially enhanced synaptic current, it is reasonable to estimate it as 1.0% of the total value of a normal synaptic current. The parameters used for an average synaptic current are 1 nA peak and 4 ms time constant of exponential decay (Vyklicky et al., 1991). The rise time of the current is very fast compared to the

Fig. 2. Lithium concentration dynamics determined by spine geometry. Computer simulations of lithium distribution in the dendritic spines during synaptic stimulation are represented for three different spine geometries. The lithium concentration is displayed in three-dimensional plots as functions of the distance from the synapse and time. Calculations were based on the separation of the space into seven segments of 0.2 μm length each. The lithium component of one current pulse was assumed to be a 10 pA spike with a 4 ms decay constant corresponding to 1% of the total synaptic current in the presence of 1 mM extracellular lithium. Intracellular lithium was assumed to be 0.5 mM in the resting state. These simulations were run for a series of seven input pulses occurring at the apical site indicated by the arrows. (A) If the spine is modeled as a simple cylinder, the lithium concentration in the head oscillates between 0.6 and 1.2 mM and follows the kinetics of the input currents. (B) If a prototypical spine (10) is considered, then lithium concentrations reach a plateau elevation several times larger than is predicted for the simple shaft model and the kinetics of decline are slower. (C) A constriction of the neck is equivalent to the diffusion barriers that may be present in mature spines. In this case, elevations in intracellular lithium are predicted that would profoundly inhibit a wide range of second-messenger mediated signals.

decay time, and therefore it has almost no effect on the charge transferred by the current during this period. Thus, the lowest estimation of the average lithium component of a synaptic inward current can be described by the exponent, $10pA \cdot \exp(-t/4ms)$.

Under these conditions, our mathematical simulation of lithium diffusion in the dendritic spine (diameters: head 0.6 μm, neck 0.2 μm) suggests that one synaptic current with a 1 nA peak and 4 ms decay time constant can increase lithium concentration in the spine head by 2 mM and in the spine neck by 1 mM. This change in lithium concentration is maintained with a decay time constant of about 6 ms. Application of two or more current spikes to the same spine at 10 ms intervals results in an oscillation of lithium concentration in the head at concentrations between 3 and 4 mM (Fig. 2B). Mature spines are often observed to have constricted necks (Spacek and Harris, 1997) which would further restrict diffusion (Figure 2C), producing oscillations in the head between 6 and 8 mM with an increased time constant of decay in the range of 15–20 ms. The presence of the spine apparatus (Wickens, 1988) might also have a similar effect on diffusion in spines without the presence of an identifiable constriction.

These data show that lithium carried through glutamate channels can cause elevations in lithium concentration sufficient to inhibit the local processing of second messenger systems in the spine during synaptic activity. These results may directly relate to a potential impact on neuronal plasticity, since the coincidence detection involved with processes such as long-term potentiation and long-term depression appear to operate on a synapse-specific basis.

Lithium levels in the cell body

If the local elevation in lithium is projected for a synapse located on the cell body, no significant change is predicted. That is, for a similar size synaptic current, less than 0.1 mM increase in local lithium concentration is predicted within 1 μm of the synapse (Fig. 3). Note that to accommodate the large volume of the cell, the size of the segments (1 μm) in this simulation is larger than for the spine simulations (0.2 μm). The local elevations immediately under the membrane at a somatic synapse would be similar to those represented for the shaft model in Figure 2A, except that for the synapse on the soma there would be an additional factor associated with the lateral diffusion.

In order to assess the relative effect of lithium flux through sodium channels as compared to our simulations of glutamate-gated lithium in synaptic spines, we made a calculation of the amount of lithium that would be predicted to be carried as part of the sodium current of a single action potential. We based our calculation on the surface area and volume of a soma approximated as a cylinder 20 microns in diameter and length. We assumed a sodium current density of 50 pA/pF and a membrane capacitance of 1 $\mu F/cm^2$. Based on the therapeutic mole-fraction of lithium, we assumed the lithium influx to be 1% of a total sodium current estimated as a square pulse of 1 ms duration. Our calculations indicate that an action potential would cause a net increase in lithium concentration in the soma of no more than 10–20 nM, several orders of magnitude less than the average increase predicted for the perisynaptic section of any the spine geometries illustrated in Figure 2. Even if one ignores steady-state efflux, a thousand or more action potentials would have only a negligible effect on lithium concentration in the neuronal soma.

DISCUSSION

Based on our data, we see that the concept of a spatial lithium microdomain may be realized in normal dendritic spines. The geometry of the spine is a sufficient factor to cause increases in the local lithium concentration of up to several millimolar. Submembrane fuzzy space (Wendt-Gallitelli et al., 1993; Carmeliet, 1992) may have additional effects on ion concentrations near the membrane, which would further amplify the potential for local modulation of signal transduction. The changes in lithium concentration associated with synaptic activity would define the limited domains of enhanced lithium effects in the precise locales of the active synapses. Therefore, the specificity of lithium's action in bipolar disorder may arise from the selective targeting of highly active synaptic sites of glutamatergic transmission with focal increases in intracellular lithium, resulting in an alteration in neuromodulatory (i.e., associative) processes of coincidence detection mediated by G-protein-coupled receptors.

The concept of coincidence detection (Konnerth, 1996) is fundamental to models of neuronal plasticity and has largely grown out of Hebb's proposal that active synapses should be selectively strengthened by processes which couple high levels of synaptic activity to cellular mediators that detect and respond to that activity. The effect of such cellular coincidence detection is to stimulate changes in either postsynaptic or presynaptic processes that selectively strengthen those active synapses. If in bipolar disorder some forms of coincidence detection become dysregulated, then lithium may selectively improve this defect by altering the coupling efficiency in a synapse-specific manner.

There are multiple modes for the generation of coincidence detection, as well as multiple potential intracellular mediators and retrograde signals. A common theme for most models of coincidence detection is the co-occurrence of depolarization, mediated by rapid-acting ligand-gated ion channels, and second messenger signals. In the CNS, the depolarization is mainly mediated by glutamate-activated ion channels (i.e., ionotropic glutamate receptors), primarily those of the

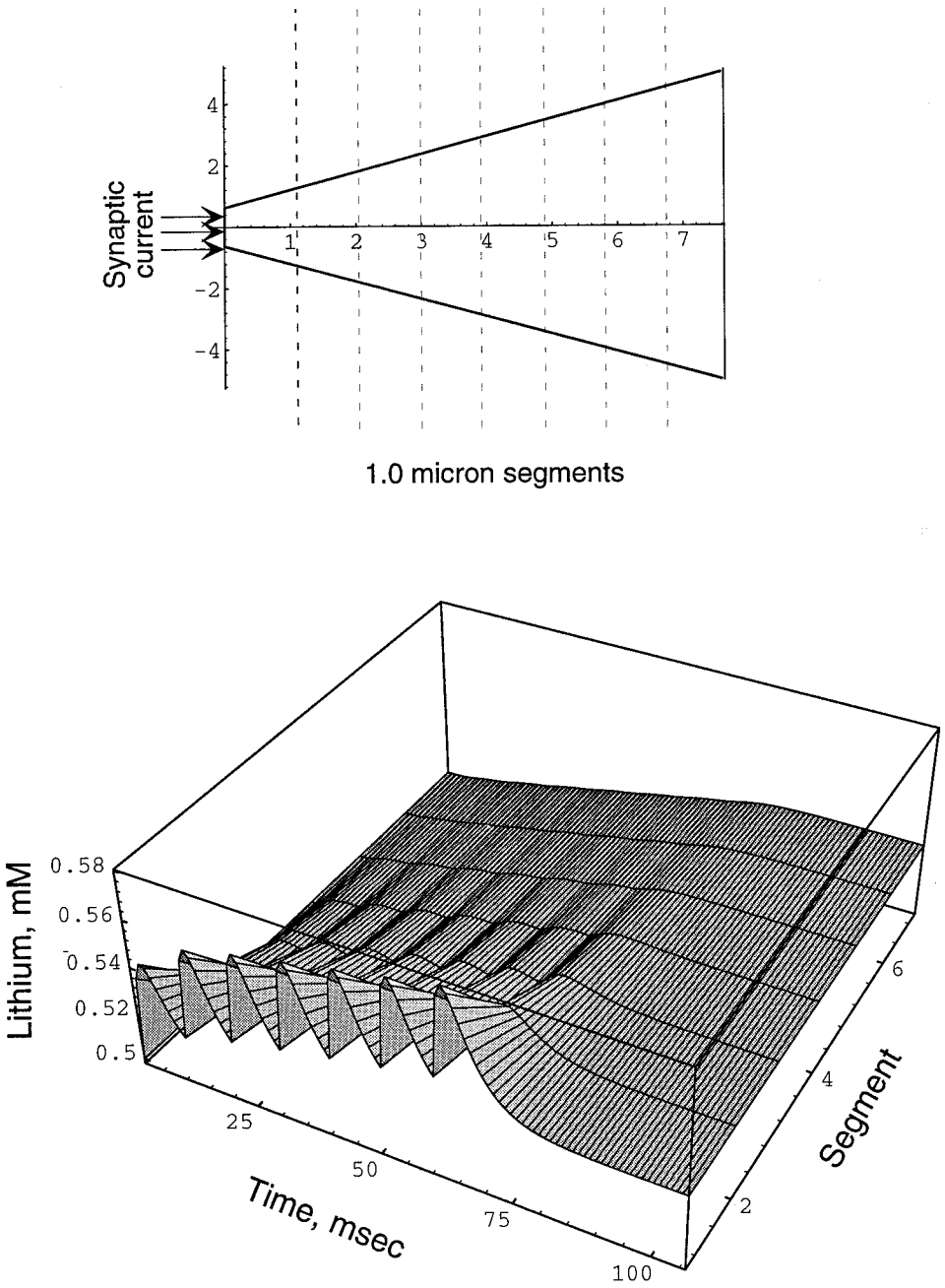

Fig. 3. Small changes in lithium concentration are predicted for synapses on the cell body. The cell was modeled as a simple cone at the indicated scale, and due to the decrease in the surface area to volume ratio, very little increase in lithium is predicted across the whole cell. Note that fluctuations will occur directly under the membrane at the synaptic site (similar to Fig. 2A), but the fluctuations will be small and dissipate rapidly due to diffusion into the open intracellular space.

AMPA/kainate class. Within the category of AMPA/kainate-activated glutamate receptors, there are many receptor subtypes which differ in their biophysical properties and have unique distributions in the brain. One way in which glutamate receptor subtypes differ is in their functional properties in the presence of lithium.

Once a depolarization occurs, there are multiple ways in which that activity can be coupled to second messenger signaling so as to produce long-term effects. One form of coupling is through a second major type of ionotropic glutamate receptor, the NMDA subtype. These receptors selectively stimulate a direct calcium signal under the condition of membrane depolarization. This special property of conditional activation is associated with a voltage-dependent block of current by extracellular magnesium, which is relieved once other

inputs have depolarized the cell. Another form of coupling is through the simultaneous activation of metabotropic glutamate receptors (mGluRs) along with the ion channel-containing glutamate receptors. These mGluRs are G-protein-coupled receptors that couple to either adenylate cyclase and cAMP production or PI turnover and the release of calcium from intracellular stores.

It has also been shown that coincidence detection may be further amplified within the cell by synergy among multiple forms of these intracellular signals. For example, calcium influx from ion channels will potentiate the IP_3-stimulated release from intracellular stores, since calcium itself functions as a co-agonist on IP_3 receptors. Likewise, the activation of adenylate cyclase will be modulated by changes in intracellular calcium.

Although sodium channels will transport lithium into neuronal soma, their influence on lithium homeostasis in the bulk cytoplasm will be negligible. Moreover, it is unlikely that lithium conduction associated with the all-or-none processes of action potentials could have the same capacity to influence coincidence detection as lithium flux through synaptic channels, since coincidence detection must operate in a synapse-selective manner. It is through microheterogeneity in intracellular lithium at the level of the synaptic locale that this ion could modulate such long-term processes as LTP and LTD, which in turn may reflect parallel neuroplastic changes implicated in the therapeutic action of lithium in stabilizing the course of manic-depressive illness (Lenox et al., 1997; Lenox and Watson, 1994).

The underlying pathophysiology of bipolar disorder is thought to be related to a dysregulation of neurotransmitter system pathways in the brain (Manji et al., 1995). Glutamate receptors are the primary mediators of synaptic excitation in the brain and so represent potentially important targets for lithium action. Our data have confirmed that synaptic transmission through ligand-gated ion channels can provide a mechanism by which lithium may alter the balance of neurotransmitter activity in critical regions of the brain and achieve both its therapeutic efficacy and specificity in the treatment of bipolar disorder.

MATERIALS AND METHODS

Electrophysiology

Oocyte and RNA preparation

RNA transcribed in vitro from cDNA clones was injected into Xenopus oocytes (Boulter et al., 1987). The RNA was stored at −80°C as a concentrated stock in DEPC water.

Two-electrode voltage clamp

Data was obtained by means of two-electrode voltage clamp recording. Recordings were made at room temperature (21–24°C) in frog Ringer (115 mM NaCl, 10 mM HEPES, 2.5 mM KCl, and 1.8 mM $CaCl_2$, pH 7.3) with 1 μM atropine. Solutions were checked for osmolarity using a Fisher Model 5001 osmometer. Voltage electrodes were filled with 3M KCl, and to reduce Ca^{+2}-dependent chloride currents, current electrodes were filled with 250 mM CsCl, 250 mM CsF, and 100 mM EGTA (pH 7.3). The resistance of voltage electrodes was between 3 and 9 MΩ, and current electrodes were between 0.5 and 3 MΩ, usually around 1 MΩ.

Bath solution and drug applications were delivered through a linear perfusion system to oocytes placed in a Lucite chamber with a total volume of 0.5 ml. A Mariotte flask filled with Ringer was used to maintain a constant hydrostatic pressure for drug deliveries and washes. Current responses were recorded on a Macintosh computer using National Instruments analog-to-digital conversion system with LabView or pClamp (Axon Instruments) software.

Current–Voltage Relationships

In order to evaluate the relative lithium permeability, 100 mV voltage ramps (from −50 to +50) of 5 sec duration were applied during the plateau phase of a prolonged agonist response. By recording the current responses to the same voltage ramp applied in the absence of glutamate, membrane responses not associated with the activation of glutamate receptors was subtracted out. The glutamate receptor current–voltage relationships thus obtained were used for reversal potential and macroscopic conductance calculations.

Mathematical model

Geometry of the spine

The spine geometry may be represented as two primary compartments: a head modeled as a sphere (diameter 0.6 μm) and a neck modeled as a cylinder (diameter 0.2 μm and length 0.7 μm) (Barbour et al., 1994; Spacek and Harris, 1997). To decrease the computation time with Mathematica® to several hours, we simplified the spine geometry to seven segments with radial symmetry (Fig. 2). Thus, the head is represented by three segments where the middle one has the same diameter as the sphere (i.e., 0.6 μm), and the neck is represented by four additional segments. In our simulations, adjustments were made in the geometry of the spine by changing the diameters of the eight disks that define the bounds of the segments.

Diffusion flux calculations

Diffusion is a three-dimensional process. But the average lithium concentration in the spine head (segments) is determined by one-dimensional diffusion from the synapse area through the head and neck to the dendrite body. Thus, the concentration is a function,

c(x,t), of two independent variables, distance from synapse (x) and time (t). In accordance with Fick's law, the concentration changes may be described by the second order partial differential equation:

$$\frac{\partial c(x,t)}{\partial t} = D \frac{\partial^2 c(x,t)}{\partial x^2}$$

The boundary condition on the left (x = 0 μm) was determined by the lithium component of the synaptic current on the left side of the first segment. The lithium efflux on the right side (x = 1.4 μm) was determined by the difference between the last segment concentration and an assumed constant concentration (0.5 mM) in the dendrite body. The differential equation for concentration (c_j) in any intermediate j-segment was presented as the following:

$$\frac{dc_j(t)}{dt} = D \frac{S_j(c_{j-1} - c_j) + S_j + 1(c_{j+1} - c_j)}{\Delta x \cdot V_j}$$

where $D = 1.03 \cdot 10^{-5}$ cm^2/s, the diffusion coefficient for lithium (Hille, 1992); S_j = area of the left side surface of the j-segment; $\Delta x = 0.2$ μm, the length of each segment, and V_j = volume of the j-segment.

The system of seven differential equations was solved and presented by using Mathematica (Wolfram Research, Inc., Champaign, IL).

ACKNOWLEDGMENTS

Technical assistance was provided by Amy Poirier and Hugo Lotti. We thank Drs. Steve Heinemann and Jim Boulter for the glutamate receptor subunit genes and Drs. Robert Oswald and Mike King for helpful comments.

REFERENCES

Barbour, B., Keller, B.U., Llano, I., and Marty, A.I. (1994) Prolonged presence of glutamate during exciatory synaptic transmission to cerebellar Purkinje cells. Neuron, 12:1331–1343.

Boulter, J., Connolly, J., Deneris, E., Goldman, D., Heinemann, S., and Patrick, J. (1987) Functional expression of two neural nicotinic acetylcholine receptors from cDNA clones identifies a gene family. Proc. Natl. Acad. Sci. USA, 84:7763–7767.

Carmeliet, E. (1992) A fuzzy subsarcolemmal space for intracellular Na+ in cardiac cells? Cardiovas. Res., 26:433–442.

Ebstein, R.P., Hermoni, M., and Belmaker, R.H. (1980) The effect of lithium on noradrenaline-induced cyclic AMP accumulation in rat brain: Inhibition after chronic treatment and absence of supersensitivity. J. Pharmacol. Exp. Ther., 213(1):161–167.

Gani, D., Downes, C.P., Batty, I., and Bramham, J. (1993) Lithium and myo-inositol homeostasis. Biochem. Biophys. Acta, 1177:253–269.

Gelenberg, A.J., Kane, J.M., Keller, M.B., Lavori, P., Rosenbaum, J.F., Cole, K., and Lavelle, J. (1989) Comparison of standard and low serum levels of lithium for maintenance treatment of bipolar disorder. N. Engl. J. Med., 321(22):1489–1493.

Hallcher, L.M., and Sherman, W.R. (1980) The effects of lithium ion and other agents on the activity of myo-inositol-1-phosphatase from bovine brain. J. Biol. Chem., 255(22):10896–10901.

Hille, B. (1992) Ion Channels of Excitable Membranes, Second Ed. Sinauer Associates, Inc., Sunderland, MA.

Kabakov, A.Y., Karkanias, N.B., and Papke, R.L. (1997) Estimation of Lithium Diffusion Dendritic Spines During Activation of Glutamate Receptors. Biophys. J., 72(2):A118.

Kanba, S., Yagi, G., Nakaki, T., Kato, R., and Richelson, E. (1991) Potentiation by a sodium channel activator of effects of lithium ion on cyclic AMP, cyclic GMP and inositol phosphates. Neuropharmacology, 30(5):497–500.

Karkanias, N.B., Lenox, R.H., and Papke, R.L. (1995) Interactions between lithium and neuronal nicotinic receptors: Potential significance for the clinical use of lithium. 25th Annual Meeting of the Society for Neuroscience. 33:19.

Keller, M.B., and Baker, L.A. (1991) Bipolar disorder: Epidemiology, course, diagnosis, and treatment. Bull. Menninger Clin., 55(2):172–181.

Konnerth, A., Tsien, R.Y., Mikoshiba, K., and Altman, J., Eds. (1996) Coincidence Detection in the Nervous System. HFSP, Strasbourg.

Lam, H.R., and Christensen, S. (1992) Regional and subcellular localization of Li+ and other cations in the rat brain following long-term lithium administration. J. Neurochem., 59(4):1372–1380.

Lenox, R.H., and Manji, H.K. (1995) Lithium. In: Textbook of Psychopharmacology. American Psychiatric Press, New York. pp. 303–349.

Lenox, R.H., and Watson, D.G. (1994) Lithium and the brain: A psychopharmacological strategy to a molecular basis for manic depressive illness. Clin. Chem., 40(2):309–314.

Lenox, R.H., McNamara, R.K., Papke, R.L., and Manji, H. (1997) Neurobiology of lithium: An update. J. Clin. Psych., in press.

Manji, H.L., Potter, W.Z., and Lenox, R.H. (1995) Signal transduction pathways: Molecular targets for lithium's action. Arch. Gen. Psychiatry, 52:531–543.

Spacek, J., and Harris, K.M. (1997) Three-dimensional organization of smooth endoplasmic reticulum in hippocampal CA1 dendrites and dendritic spines of the immature and mature rat. J. Neurosci., 17(1):190–203.

Vyklicky, J.L., Patneau, D.K., and Mayer, M.L. (1991) Modulation of excitatory synaptic transmission by drugs that reduce desensitization at AMPA/kainate receptors. Neuron, 7(6):971–984.

Wendt-Gallitelli, M.-F., Voigt, T., and Isenberg, G. (1993) Microheterogeneity of subsarcolemmal sodium gradients. Electron probe microanalysis in guinea-pig ventricular myocytes. J. Physiol. 472:33–44.

Wickens, J. (1988) Electrically coupled but chemically isolated synapses: Dendritic spines and calcium in a rule for synaptic modification. Prog. Neurobiol. 31:507–528.